PLOS ONE

RESEARCH ARTICLE

Subjective value then confidence in human ventromedial prefrontal cortex

Allison D. Shapiro*, Scott T. Grafton

Department of Psychological and Brain Sciences, University of California, Santa Barbara, CA, United States of America

* shapiro.alli@gmail.com

OPEN ACCESS

Citation: Shapiro AD, Grafton ST (2020) Subjective value then confidence in human ventromedial prefrontal cortex. PLoS ONE 15(2): e0225617. https://doi.org/10.1371/journal.pone.0225617

Editor: Sam Gilbert, University College London, UNITED KINGDOM

Received: November 6, 2019

Accepted: January 29, 2020

Published: February 10, 2020

Data Availability Statement: Data are available from: (https://neurovault.org/collections/6321/).

Funding: This work supported by Grant W911NF-16-1-0474, Contract W911NF-09-0001 and Cooperative Agreement W911NF-19-2-0026 with the Army Research Office of the Army Research Laboratory to STG. https://www.arl.army.mil/www/default.cfm. The funders had no role in study design, data collection and analysis, decision to publish, or preparation of the manuscript.

Competing interests: The authors have declared that no competing interests exist.

Abstract

Two fundamental goals of decision making are to select actions that maximize rewards while minimizing costs and to have strong confidence in the accuracy of a judgment. Neural signatures of these two forms of value: the subjective value (SV) of choice alternatives and the value of the judgment (confidence), have both been observed in ventromedial prefrontal cortex (vmPFC). However, the relationship between these dual value signals and their relative time courses are unknown. Twenty-eight men and women underwent fMRI while performing a two-phase approach-avoidance (Ap-Av) task with mixed-outcomes of monetary rewards paired with painful shock stimuli. Neural responses were measured during offer valuation (offer phase) and choice valuation (commit phase) and analyzed with respect to observed decision outcomes, model-estimated SV and confidence. During the offer phase, vmPFC tracked SV and the decision but not confidence. During the commit phase, vmPFC tracked confidence, computed as the quadratic extension of SV, but not the offer valuation nor the decision. In fact, vmPFC responses from the commit phase were selective for confidence even for reject decisions wherein confidence and SV are inversely related. Conversely, activation of the cognitive control network, including within lateral prefrontal cortex (lPFC) and dorsal anterior cingulate cortex (dACC) was associated with ambivalence, during both the offer and commit phases. Taken together, our results reveal complementary representations in vmPFC during value-based decision making that temporally dissociate such that offer valuation (SV) emerges before decision valuation (confidence).

Introduction

Every day, we navigate a maze of choices, guided by our subjective preferences and goals. When the route forks, multiple forms of value imbue the selection of one's path. We assess the value of potential actions from their relative costs and benefits, as well as the value of our own judgment–accurate decisions are valuable decisions, regardless of the options.

Much progress has been made toward understanding how the brain resolves value-based decisions [1, 2]. vmPFC, in particular, is crucial for integrating reward and cost attributes of choice alternatives [3–6] and automatically tracking subjective value (SV)[7], which is the perceived utility of objective value information relative to the decision maker's preferences and goals[7, 8]. Neuroeconomic models benefit from mixed-outcome ApAv tasks, which pose realistic, consequential

choice scenarios (e.g. accept or reject offers of appetitive rewards contingent on aversive costs). Such fMRI studies in humans demonstrate multiple value representations in vmPFC including rewards, decision variables, SV, and the valuation models that inform SV [9–12].

Recent research suggests that vmPFC also signals choice confidence, how strongly one can believe they are making the best decision. For example, vmPFC activation varies with confidence about perceptual judgments [13–15] and lesions lead to atypical confidence reports on general knowledge tests [16] These findings could be evidence that vmPFC performs a valuation of one's judgment, assigning high value to high confidence decisions [17]. Confidence signals in vmPFC also accompany value-based decisions [17–19], which is intriguing given the relationship between confidence and value. Self-reported confidence takes a U-shaped function with respect to first-order valuation judgments [7, 20]: decisions about extremely high- or low-value items elicit stronger confidence than decisions about items with neutral or ambiguous value. Similarly, vmPFC responses take a U-shaped function with respect to value in risky decision making [21]. Accordingly, Lebreton et al. [17] operationalized confidence as the quadratic extension of value and elegantly demonstrated that vmPFC tracks modeled confidence, even in the absence of explicit ratings.

Given this literature, vmPFC should track both SV and its quadratic extension, confidence, in mixed-outcome ApAv decision making, but this has not been explicitly tested. Specifically, confidence about accept choices (typically positive SV) should increase as SV increases whereas confidence about reject choices (typically negative SV) should increase as SV decreases. It is unknown how vmPFC represents both SV and confidence in value-based choices, particularly when confidence and value are inversely related (i.e. during decisions to reject). One possibility is that confidence evolves in parallel with decision variables [22] and the two signals are either integrated within a region or are represented in separate neuroanatomical substrates. In line with this hypothesis, early confidence-related signals have been recorded from frontal and parietal sites [23, 24], including vmPFC [7, 14, 19]. Alternatively, confidence and SV may have different time courses such that confidence evolves relatively later during retrospective metacognitive judgments or continued deliberation after choice commitment [25–29], both of which can recruit medial prefrontal cortex [30–32].

To test this, we deployed a two-phase ApAv task in which participants accepted or rejected offers of monetary rewards paired with painful shock stimuli. BOLD responses were measured during offer valuation (offer phase) and choice valuation (commit phase). Observed decision outcomes and model-based estimates of SV and confidence were used to predict neural activity in vmPFC and throughout the brain during both phases of decision making.

Methods

Experimental design

Participants. We report the data from 28 paid volunteers that participated in the study (17 women, 27 right-handed, mean age = 21.9, sd = 2.8). One additional participant completed the study but was removed from analyses due to significant susceptibility artifacts causing excessive errors in spatial normalization. No participants had a history of neurological injuries or illnesses or current daily use of psychoactive medications. All participants provided written consent to this research protocol that was approved by the Institutional Review Board at the University of California, Santa Barbara.

Session overview. All testing was performed on the same day. Participants first provided informed consent and were screened for disqualifying criteria. Because our task entailed ApAv decisions with pain stimuli, participants next underwent a pain thresholding procedure and were familiarized with the mapping between experimental stimuli and the pain intensities they

represented. Then, participants performed the decision making task while in the MRI scanner. Finally, after they had completed all experimental tasks and been removed from the scanner, participants received the pain stimuli and monetary rewards associated with the choices they made during the task.

Pain thresholding procedure. We used mild cutaneous electrical shocks as pain stimuli. Pain thresholding allowed us to control for individual differences in pain tolerance for electrical shocks such that a given experimental stimulus was associated with the same subjective experience of pain across participants. To identify participant-specific minimum and maximum shock intensities, participants completed a pain thresholding procedure before the decision-making task, outside of the MRI scanner. Electrical shocks were administered with a constant current stimulator (Digitimer DS7A, Digitimer, Great Britain) controlled by a train generator (DG2A Train/Delay Generator, Digitimer, Great Britain). Each shock had a duration of 1 s and a frequency of 100 Hz with a 2 ms waveform. Two adhesive electrodes were placed on the back of the participant's hand approximately 1 inch above the wrist and connected to the stimulator. When a shock was administered, electric current was run between the two electrodes, causing an aversive sensation that is increasingly painful at higher levels of current.

The first stage of thresholding was a ramp-up procedure in which the experimenter delivered several shocks, each time increasing the intensity by 1 mV. The participant was instructed to report three thresholds: the lowest intensity at which they detected the shock, the lowest intensity at which the shock caused discomfort, and the intensity at which the shock became unbearably painful. The second stage was a rating procedure in which the participant received fourteen shocks with intensities between the discomfort threshold and unbearable threshold and rated the pain from each on a 0–10 scale. Next, both the ramping and rating stages were repeated to verify that we had accurately identified the participant's pain tolerance. Finally, the pain ratings and shock intensities from the second rating procedure were fit with a sigmoid function to model the relationship between shock intensity and perceived pain for this individual[33]. Based on this sigmoid function, we identified the shock intensity that predicted a pain rating of 8 out of 10. No payout trials during the decision task had costs exceeding this value.

Familiarization procedure. Before the decision making task, participants were shown five example offer stimuli illustrating costs of 5%, 25%, 50%, 75% and 95% while the experimenter delivered a shock at the corresponding intensity relative to their discomfort and maximum pain thresholds (with 0% = minimal discomfort and 100% = maximal pain). Participants were instructed to remember the sensation associated with the example shocks and use these as points of reference when making choices during the task and that the real offers would include shocks anywhere within the range of intensities, not only at the example levels.

ApAv task

Offer stimuli. We adapted an approach–avoidance task similar that implemented in non-human primates by Amemori and Graybiel [4, 34] in which participants accepted or rejected offers with mixed appetitive and aversive outcomes. On each trial, the participant was offered a certain amount of money in exchange for receiving a shock of a certain intensity (Fig 1A). The participant chose either to accept *both* the money and the shock or reject both (i.e. receiving a monetary reward was always contingent on also receiving its associated cost). Therefore, trial stimuli were deterministic mixed-outcome choice scenarios as there were no manipulations involving probabilistic chances or risks of receiving the shock and/or money that could be used to form decision strategies.

The offer stimuli were two horizontal bars, one had an overlaid $ symbol and illustrated the offered reward and the other had an overlaid lightning bolt symbol and illustrated the

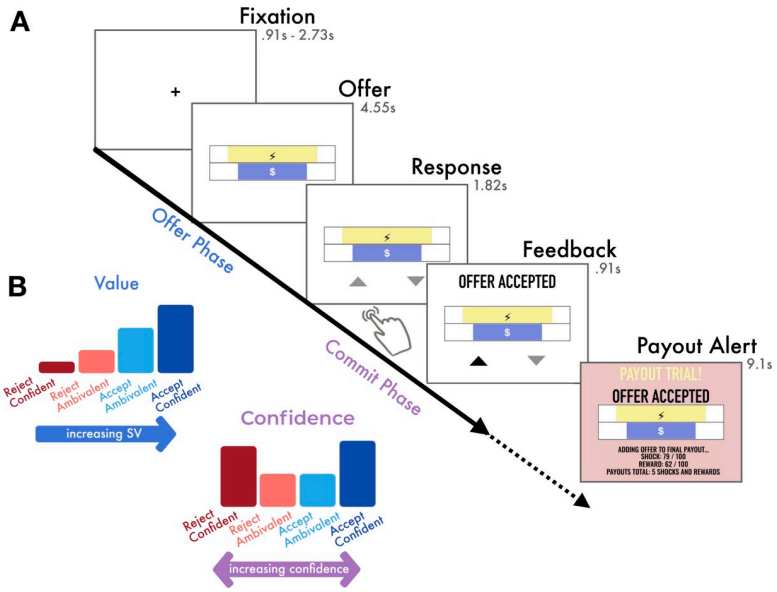

Fig 1. Experimental task and variables of interest. (A) Experimental Task: On each trial, the participant was offered one monetary reward ($ bar width represents amount, ranging continuously $0.01-$1.50) contingent on enduring 1 painful shock (lightning bolt bar width represents pain intensity, ranging continuously from minimally to maximally painful). Participants were instructed to use the offer phase to evaluate the offer and to decide if they would accept or reject it, but they were not yet able to respond. During the commit phase, response mappings appeared and participants made a left or right button press according to the location of the triangle representing their choice (up triangle = accept, down triangle = reject), which varied randomly between trials to prevent preparation of motor responses during the offer phase. After submitting a response, the corresponding triangle was highlighted. Finally, feedback indicating whether the offer was accepted or rejected was added. On payout trials (10 random trials of 189 total), a payout alert followed the feedback. If the participant had accepted the offer, they would receive the monetary reward and also endure the shock at the end of the task, otherwise the participant would receive neither. **(B)** Illustration of variables of interest: We were interested in two types of value inherent in economic decision making: the perceived value of the offer stimulus (SV) accounting for its cost and reward attributes, and the value of one's judgment (confidence), which measures the extent to which one believes they are making the best decision. For accept decisions (blue bars), there is a positive relationship between SV and confidence: as SV increases, one becomes increasingly confident that accepting the offer is the best decision. However, for reject decisions (red bars), there is an inverse relationship between SV and confidence: one becomes increasingly confident about rejecting offers as SV *decreases*. We tested whether they are evaluated simultaneously or whether they have a temporal order within the course of decision making.

https://doi.org/10.1371/journal.pone.0225617.g001

contingent cost. The width of the bars represented the amount of each attribute being offered on the current trial, with monetary rewards ranging continuously from $0.01 to $1.50 and shock intensities ranging continuously from minimal discomfort to maximal pain. Each bar was within a larger rectangular frame that illustrated the maximum possible bar width. The bars were blue and yellow, and color-attribute mappings varied between participants. The relative position of the cost and reward bars (i.e. which bar was above the other) alternated between blocks. The offer stimuli were centrally aligned and stacked just above and just below the vertical midpoint of the display. Overall, there were 189 unique offers, each presented as a single trial, unless the participant failed to respond, in which case the offer was repeated at the end of the experiment. Trials were split between six functional runs, with each run containing 31 or 32 trials. All participants viewed the same set of offers, presented in the same pseudo-random order that systematically covered all quadrants of the decision space.

Decision making task. On each trial, the participant first saw a fixation point in the center of the screen for either 910 ms, 1820 ms or 2730 ms, randomly varied between trials. Then, the offer stimulus was shown for 4550 ms. The participant was instructed to use this time to evaluate the offer but could not yet indicate a choice. Next, the offer remained on the screen and

two response mappings appeared in left and right positions beneath the offer stimulus for 1820 ms. During this time, the participant was required to respond with a button press, indicating their commitment to either accept (approach) or reject (avoid) the offer. All stimuli remained on the screen for the remainder of the response interval, and after the response was submitted, the response mapping corresponding to their choice was highlighted. Participants were allowed to change their response within the 1820 ms response interval. The response mappings were an upward pointing triangle representing the accept option and a downward pointing triangle representing the reject option. The participant used either the index or middle finger of their right hand to press either the left or right (respectively) button on a Cedrus LP-RH response pad transmitting through a Lumina LSC-400 controller (Lumina, Cedrus Corportation, San Pedro, CA, USA), according to the location of their preferred choice option. The left/right positions of the choice options varied from trial to trial, preventing the participant from pre-planning a motor response before the response phase. Finally, a 910 ms feedback interval followed the response interval. Feedback included the offer stimulus, which remained on the display, and text stating whether the offer was accepted or rejected. On payout trials an additional 9100 ms payout alert followed the decision feedback.

Because we were interested in value-processing during different phases of decision making, our analyses separately analyzed neural responses from the offer phase and the commit phase of each trial. The offer phase was the 4550 ms in which the offer was displayed but the participant was not yet able to submit a response. The commit phase was the 2730 ms comprising the response interval (1820 ms) and the feedback interval (910 ms).

Payouts. Participants did not receive the rewards and shocks for all accepted trials. Instead, during trial generation, 10 pseudorandomly selected offers were tagged as payout trials. On these trials, if the participant accepted the offer the payout alert indicated that they would receive both the monetary reward and the shock. If they rejected the offer, the payout alert indicated they would receive neither. The payout alert also showed the cumulative number of payouts accepted so far. Participants were encouraged to assume that every trial was a payout offer and decide to accept or reject it accordingly, as they would not see the payout alert until after they'd submitted their choice. Although participants were notified whether an offer was a payout immediately after choosing to accept or reject it, the actual delivery of monetary rewards and shocks from payout trials occurred after they had completed the entire decision making task and had been removed from the MRI scanner. In pilot studies, we found that providing realtime payout feedback, relative to showing which trials were payouts at the end of a fixed-length block or at the end of the task, reduced the proportion of offers that were accepted. We believe that this may indicate that instant feedback reduces temporal discounting of future costs, relative to when that information is delayed, even though in both cases the actual costs would be delivered after the entire task.

All participants also performed an additional cost-benefit decision making task after they completed the approach-avoidance task, the results of which are not reported here. Twenty-four of the participants also underwent simultaneous physiological recordings of impedance cardiography while performing the decision making tasks in the MRI scanner, impedance cardiography data is also not included here.

Behavioral statistical analysis

Estimating SV from decision behavior. The subjective value (SV) of each offer can be represented as

$$SV = \beta_0 + \beta_r r_{offer} + \beta_s s_{offer}$$

where r_{offer} is the available reward, s_{offer} is the contingent shock, β_r and β_s describe how strongly

the individual subject weights rewards and shocks, and β_0 is the individual's intercept, indicating their intrinsic motivations to pursue reward versus avoid shock (33). We separately modeled each participant's choice data with logistic regression, a specialized from of the generalized linear model, using the glm package in R. Offers to which participants failed to respond before the decision deadline were repeated at the end of the task. Choice outcomes from the second presentation were included in the dataset used for generating valuation models but these trials were excluded from the fMRI analysis. Participant-level models were used inversely to estimate the perceived subjective value of each offer, SV, and the likelihood that it would be accepted, P(Acc) specific to each individual on each trial.

$$SV = \beta_0 + \beta_r r_{offer} + \beta_s s_{offer} = log\frac{P(Acc)}{1 - P(Acc)}$$

$$P(Acc) = \frac{1}{1 + e^{-SV}}$$

Estimating confidence from SV. Here, we operationalize choice confidence as the extent to which one can believe they are making the best decision. In our task, given the options to either accept or reject, the best choice depends on the perceived value of the offer and consequently choice confidence is maximized when SV unambiguously points to one choice over the other. Therefore, confidence varies in a U-shaped function with respect to increasing SV such that when SV is extremely high or extremely low, one can be highly confident in choices to accept or reject the offer, respectively. When an offer's SV is neutral there is more ambivalence about the decision (Fig 1B). We quantify confidence in accordance with Lebreton et al. [17], who operationalized decision confidence as the quadratic extension of perceived value, and were therefore able to estimate trial-wise confidence in the absence of explicit confidence ratings.

$$Confidence = SV^2$$

We used these trial-by-trial estimates to test whether behavioral response times and neural activity varied with respect to choice confidence. Notably, because we did not collect metacognitive self-reported confidence ratings, we do not intend to make explicit claims about the subjective experience of confidence. Previous research has found mixed results regarding how closely model-estimated confidence varies with self-reported confidence, see the discussion for a further explanation. Therefore, we primarily aim to describe neural responses that vary with model-estimated confidence.

We also inspected the relationship between confidence and choice outcomes. Trials were categorized into confident accepts (AccCon), ambivalent accepts (AccAmb), confident rejects (RejCon), and ambivalent rejects (RejAmb) by binning each participant's trials into accepted and rejected trials and then performing a median split on *SV* on both bins. Accepted offers in the upper 50% SV were assigned to AccCon and the rest were assigned to AccAmb. Rejected offers in the upper 50% SV were assigned to RejAmb, and the rest were assigned to RejCon. Notably, because we observed substantial individual differences in subjective valuation, both parameterizing and categorizing the offers according to individual-level model-based estimates allowed us to describe objectively identical offers differently for each participant, according to their unique preferences. This was a critical feature of our study that allowed us to observe group-wide neural responses that were specific to decision outcome, SV, and confidence, regardless of the objective properties of the stimulus.

In our paradigm, P(Acc) varies as a sigmoidal function of SV while choice confidence varies as a U-shaped function of SV. Consequently, when P(Acc) is close to either 0 or 1 there is high choice confidence in either accepting or rejecting the offer, respectively. When P(Acc) is close to .5, there is ambivalence about committing to either choice. In a two-dimensional decision space in which reward values are represented on one dimension, cost values are represented on the other, and the modeled decision boundary is the vector along which P(Acc) = .5, the choice confidence associated with a reward-pain offer pair increases with its distance from the decision boundary. We present individual choice outcomes and binned choice confidence overlaid on estimated P(Acc) throughout the decision space.

Neuroimaging data acquisition and preprocessing

Neuroanatomical ROI. We investigated task-related involvement within an a priori region of interest (ROI), vmPFC. The ROI was anatomically defined from the Harvard-Oxford cortical structural probabilistic atlas (https://fsl.fmrib.ox.ac.uk/fsl/fslwiki/Atlases), and includes all voxels with at least 25% likelihood of being located within areas labelled Frontal Medial Cortex or Subcallosal Cortex. The rationale for selecting this rather inclusive and anatomically-defined ROI was that regions throughout vmPFC have been implicated with SV and confidence processing. We did not have a priori hypotheses regarding about anatomically specific loci within vmPFC that would be uniquely sensitive to value and confidence in our task, and therefore no basis for dividing the ROI into smaller sub-components. Instead, we extracted the most relevant regions from a commonly used atlas and applied a relatively low threshold for inclusion to ensure that we did not inadvertently exclude cortex where we might find relevant activity.

MRI protocols. Anatomical and functional MRI data were collected on a Siemens 3T Magnetom Prisma Fit with a 64-channel phased-array head and neck coil (58 channels active for functional coronal imaging). High-resolution 0.94 mm isotropic T1- (TR = 2500 ms, TE = 2.2 ms, FA = 7˚, FOV = 241 mm) and T2*-weighted (TR = 3200 ms, TE = 570 ms, FOV = 241 mm) sagittal sequence images were acquired of the whole brain. Next, functional MRI recordings were collected while participants performed the decision making task. For each functional run, a multiband T2*-weighted echo planar gradient-echo imaging sequence sensitive to BOLD contrast was acquired (TR = 910 ms, TE = 32 ms, FA = 52˚, FOV = 192 mm, multiband factor 4) provided by the Center for Magnetic Resonance Research in accordance with a current license. Each functional image consisted of 64 coronal slices acquired perpendicular to the AC-PC plane (3 mm thick; 3x3 mm in-plane resolution). Coronal orientation is necessary when acquiring simultaneous impedance cardiography to avoid artifact [35].

MRI pre-processing. Anatomical data was skull-stripped using the brain extraction script from Advanced Neuroimaging Tools (ANTs) [36]. All other image pre-processing was performed with FMRIB's Software Library (FSL, www.fmrib.ox.ac.uk/fsl). The first 10 volumes of each functional run were removed to eliminate non-equilibrium effects of magnetization occurring before the start of the task. The remaining functional volumes were skull-stripped using BET [37] motion corrected using MCFLIRT [38], spatially smoothed using a Gaussian kernel of FWHM 5mm, intensity normalized relative to the grand-mean of the entire 4D dataset by a single multiplicative factor, and underwent high-pass temporal filtering (Gaussian-weighted least-squares straight line fitting, with sigma = 50.0s).

In preparation for group analyses, participants' six functional runs were registered to their anatomical image and then to the Montreal Neurological Institute (MNI) 2mm averaged 152-brain template included with FSL distributions, using FSL's linear image registration tool

with 12 degrees of freedom (FLIRT; [38, 39]. Refinement of the latter transformation was carried out with FSL's nonlinear registration image registration tool (FNIRT) with a 10mm warp resolution [40, 41].

Neuroimaging statistical analysis

fMRI analysis. FMRI data processing was carried out using FEAT (FMRI Expert Analysis Tool) Version 6.00, part of FSL (FMRIB's Software Library, www.fmrib.ox.ac.uk/fsl). Time-series statistical analysis was carried out using FSL's improved linear model (FILM) with local autocorrelation correction [42]. We performed whole-brain statistical analyses with two general linear models (GLMs), as described below. Both GLMs had separate terms for the offer phase (off) and the choice commitment phase (com) of each trial. Offer phase regressors were time-locked to the onset of the offer and had a duration of 4.55s, during which the participant assesses the SV of the offer but cannot yet respond. Commit phase regressors were time-locked to the onset of the response mappings and had a duration of 2.73 seconds, during which the participant submits their decision about the offer and then views feedback confirming their choice. Finally, the GLMs also included a nuisance regressor for payout notifications, which were not used in analyses of interest but were intended to absorb variance in neural responses associated with subjective value (as payout notifications included an image of the payout offer) but unrelated to decision making processes. The payout regressor was time-locked to the onset of the payout notification and had a duration of 4.55 s, and the remaining 4.55 s of the payout notification screen was included with baseline activity.

Both analyses were performed at three sequential levels. First, at the run level, each participant's six runs were separately modeled to find mean within-run activity corresponding each regressor and contrast images were generated by estimating pairwise differences between conditions. Then, at the participant level, run-level data was combined (fixed effects) to find the participant's overall mean response relating to each regressor and contrast. Finally, at the group level, the participant data was combined (mixed-effects treating participant as a random effect with FSL's FLAME 1) to find the group-wide mean responses for each regressor and contrast.

We tested the results of each contrast with non-parametric permutation testing at the whole brain level with threshold-free cluster enhancement (TFCE), implemented with FSL's Randomise. This approach minimizes false positives by deriving a null distribution from the voxelwise data rather than assuming a parametric null distribution. For one-sample t tests (such as those in the present study), the distribution is created by iteratively multiplying statistical map values by 1 or -1, we performed 5,000 permutations of each contrast. TFCE detects clusters of contiguous voxels without setting an arbitrary cutoff for minimum cluster size or voxel statistic but rather summarizes the cluster-wise evidence at each voxel, against several types of cluster-forming thresholds and controls the family-wise error (FWE) rate at $p = .05$ [43, 44]. We present figures with voxel-wise T-values from all voxels that survived whole-brain TFCE correction. Some contrasts yielded significant voxels across contiguous but widespread regions of cortex, and consequently reporting only the peak voxel of a cluster would obscure other local maxima in different anatomical regions. Therefore, we also report the coordinates, t statistics, Brodmann area, and anatomical structure labels from Automated Anatomical Labelling the of the MNI atlas for local maxima within each cluster in the supplementary materials. Local maxima were found with the cluster command provided with FSL and labelled with label4MRI, a freely available toolbox for R (https://github.com/yunshiuan/label4MRI). We additionally report results from sub-conditions of GLM2 restricted to and TFCE corrected only within our primary ROI of interest, vmPFC.

GLM1: Parametric analysis SV and confidence. GLM1 was a parametric statistical analysis to observe neural activity modulated by SV and confidence (CD) during the offer and commit phases of each trial:

$$Y = \beta_{off}X_{off} + \beta_{com}X_{com} + \beta_{SVoff}X_{SVoff} + \beta_{SVcom}X_{SVcom} + \beta_{CDoff}X_{CDoff} + \beta_{CDcom}X_{CDcom} + \beta_{payout}X_{payout} + \varepsilon$$

where Y is the time series of a given voxel predicted by a design matrix with one row for each time sample and one column for each of 7 trial regressors, convolved with a canonical gamma hemodynamic response function. The model included categorical terms for baseline activation during the offer and commit phases ($\beta_{off}X_{off,}$ $\beta_{com}X_{com}$). Parametric terms $\beta_{SVoff}X_{SVoff}$ and $\beta_{CDoff}X_{CDoff}$ were both orthogonalized with respect to baseline activation during the offer phase ($\beta_{off}X_{off}$) to capture variance in neural activity during the offer phase explained by trial-by-trial SV and confidence. Likewise, $\beta_{SVcom}X_{SVcom}$ and $\beta_{CDcom}X_{CDcom}$ were orthogonalized with respect to baseline activation during the commit phase ($\beta_{com}X_{com}$) and modeled neural activity related to SV and confidence during the commit phase. The SV and confidence regressor weights were trial-wise SV and confidence values, range normalized by z-score.

Note that SV and confidence terms were orthogonalized with respect to baseline activation during the corresponding trial phase because baseline activation in itself was not a parameter of interest. Therefore, orthogonalization essentially served to mean-center SV and confidence independently at the run level. Orthogonalizing either or both of the SV and confidence terms with respect to one another could have diminished the interpretability of the parameter estimates associated with each [45].

We also examined correlations between terms in GLM1 in order to address concerns of multicollinearity. The terms of interest were the columns of predictor values in the design matrix from GLM1 corresponding to SV and confidence from the offer and commit phases (X_{SVoff}, X_{CDoff}, X_{SVcom}, X_{CDcom}). First, we estimated correlations between the two terms of interest from each trial phase ($X_{CDoff} \sim X_{SVoff}$, and $X_{CDcom} \sim X_{SVcom}$) at the run level. The R^2 values were transformed into Fisher's Z-scores and the mean Z-score across all runs and participants was transformed back to an R^2 value. Second, we estimated the variance inflation factor (VIF) for each term of interest (i), as $1/(1\text{-}R_i^2)$, where R_i^2 was the multiple R^2 from regressing the column of predictor values for the term of interest against all remaining columns in the design matrix. Then, the median VIF for each term of interest was taken across all runs and participants. Large VIFs would indicate a potentially problematic design in which multicollinearity could inflate the estimated coefficients for the terms of interest.

For the purposes of visualizing gradual changes in neural responses over the course of the trial, GLM1 was re-estimated with a finite impulse response (FIR) model. Rather than splitting the trial into two phases, neural responses tracking SV and confidence were measured at each TR (910 ms per TR) beginning at the onset of the offer stimulus. The model was identical to GLM1 except for the following modifications. Instead of two categorical regressors for the offer and payout onsets there was a single categorical regressor for the offer stimulus onset and instead of two parametric terms for both SV and confidence there was only one for each. Instead of convolving regressors with a gamma HRF, FIR basis functions sampled neural responses at each of 18 discrete time points, with the first sample taken 0 s after trial onset and the last sample taken 15.47 s after offer onset. Given the delay of the BOLD response, the 16 second window was intended to capture the full progression of neural responses that began between offer onset and the end of the trial. FIR basis functions were fit for each of the trial regressors (categorical offer regressor, parametric SV regressor, and parametric confidence regressor) as well as the payout nuisance regressor, for which the appearance of the payout

notification marked the stimulus onset. As in GLM1, these analyses were first performed at the run level and then combined at the participant level, both of which were conducted in FSL's FEAT. Participants' mean parameter estimates for SV and confidence from each of the 18 FIR times were extracted from the anatomical vmPFC ROI and used for visualization.

GLM2: Categorical choice by confidence analysis. GLM2 estimated categorical variance in neural responses during the offer and commit phases of each trial:

$$Y = \beta_{ACoff}X_{ACoff} + \beta_{AAoff}X_{AAoff} + \beta_{RCoff}X_{RCoff} + \beta_{RAoff}X_{RAoff} + \beta_{ACcom}X_{ACcom} + \beta_{AAcom}X_{AAcom} + \beta_{RCcom}X_{RCcom} + \beta_{RAcom}X_{RAcom} + \varepsilon$$

The first four terms modeled the offer phase of confident accepts, ambivalent accepts, confident rejects, and ambivalent rejects, respectively. The next four terms modeled the commit phase of the same conditions. The ninth regressor modeled payout notifications. Our contrasts compared each condition with baseline, tested main effects of choice outcome (i.e. accepted offers vs. rejected offers irrespective of choice confidence) and choice confidence (i.e. high confidence choices vs. low confidence choices irrespective of choice outcome) separately during the offer and commit phases. Select pairwise comparisons within these conditions: AccCon vs. AccAmb, and RejCon vs. RejAmb were inspected within our anatomical ROI, vmPFC.

Time courses of SV and confidence responses in vmPFC. To further characterize the pattern of vmPFC responses during the offer and commit phases, we extracted mean parameter estimates within vmPFC for each condition during each trial phase. We tested whether vmPFC simultaneously tracks value and confidence, or if these two signals have a temporal order within the decision making process. Following the logic of Lebreton et al. [17], we assumed that the shape of the function of vmPFC activation with respect to trial conditions of ascending value (RejCon < RejAmb < AccAmb < AccCon) would be indicative of the information being processed during each trial phase. A linear increase of vmPFC response magnitudes with respect to offer value would suggest SV processing, whereas a quadratic function would suggest confidence processing. If vmPFC simultaneously tracked confidence and value, model terms for both the linear and quadratic extensions of value would be necessary to fully explain the observed pattern of vmPFC activity.

To tailor the predictors in these models to individual participants, we used the mean perceived value across trials from each condition, calculated separately for each participant. SV varies substantially between participants depending on the consistency of their choice behavior as slight changes in choice consistency cause substantial changes in participants' model-estimated SV predictors. Consequently, there was a large range of SV and SV^2 throughout the group and many participants' data only spanned only a portion of that range, making it difficult to draw conclusions at the group level. P(Acc) and P(Rej) (the latter is equivalent to 1-P(Acc)) are always restricted to the range of 0 to 1. Consequently, P(Acc)-P(Rej) normalizes value to range from -1 to 1 while preserving the sign of SV, with negative values predicting reject choices, positive values predicting accept choices, and values surrounding zero indicating decision ambivalence. Furthermore, whereas in GLM1 we measured parametric modulation by SV, in GLM2 trials were binned according to observed choice, which is more specifically related to P(Acc)-P(Rej). Therefore, we used P(Acc)-P(Rej) as value predictors in our ROI analysis, which improved consistency for groupwide analysis while retaining the sign of SV. Previous research has used a similar approach [17].

Each participant's mean vmPFC parameter estimates from the four trial conditions were predicted as a function of the mean P(Acc)-P(Rej) of that condition using linear mixed effects

regression, implemented with the lme4 package for R [46].

$$\text{Linear Model}: \ \bar{y} = b_0 + b_1(P(Acc) - P(Rej)) + \varepsilon$$

$$\text{Quadratic Model}: \ \bar{y} = b_0 + b_1(P(Acc) - P(Rej)) + b_2(P(Acc) - P(Rej))^2 + \varepsilon$$

The linear and quadratic extensions of P(Acc)-P(Rej) were specified as fixed effects and we included a random effect on the model intercept across subjects to account for baseline variation in vmPFC parameter estimates. Predictor values entered into the model were participants' mean P(Acc)-P(Rej) of trials from each of the four conditions. Both models were separately fit to parameter estimates of BOLD responses in vmPFC during the offer phase and during the commit phase. Due to ambiguity in estimating denominator degrees of freedom, linear mixed model fits are not best evaluated by p-values. However, significance can be inferred from confidence intervals constructed by iteratively sampling the model posterior to estimate the likelihood of the observed parameter estimates. We ran 5,000 simulations using the posterior distributions over each parameter from the mixed models using the merTools package for R. We report significant parameters with 95% CIs that do not span zero. For interested readers, corresponding p-values estimated with Satterthwaite's method implemented in the lmerTest package for R are also provided. Model comparison (ordinary likelihood ratio test) and relative AIC and BIC values were used to determine the best fitting model for the offer phase and for the commit phase.

Temporally restricted value and confidence signals in vmPFC. As a stronger test for temporally-restricted value and confidence representations in vmPFC, we conducted a conjunction analysis to identify whether there were common voxels within vmPFC that preferentially responded both to positive value during the offer phase and to confidence during the commit phase. The set of voxels with this characteristic would have stronger responses to accept decisions (AccAmb + AccCon) than to reject decisions (RejAmb + RejCon) during the offer phase, and stronger responses to confident decisions (AccCon + RejCon) than to ambivalent decisions (AccAmb + RejAmb) during the commit phase. Eliminating the trial types that were common to both decision phases on the same side of the contrast leaves the set of voxels with AccAmb > RejCon during the offer phase and RejCon > AccAmb during the commit phase. We took the conjunction of voxels where both of these contrasts were statistically significant (surviving TFCE correction within vmPFC).

Behavioral correlates of SV and confidence

We aimed to measure neural correlates of implicit, naturalistic experiences of confidence during decision making. Therefore, our task did not solicit metacognitive confidence ratings. We estimated confidence as the quadratic extension of value in accordance with a similar study that validated this operationalization by demonstrating that both response times (RTs) and self-reported confidence were related by the *inverse* quadratic to value, and thus RTs and confidence were negatively correlated. Notably, that study found that the quadratic extension of value (i.e. model-based confidence) better predicted self-reported confidence than RTs, suggesting that while RTs were a useful behavioral correlate of subjective confidence, they didn't fully explain variance in metacognitive confidence ratings [7, 17]. Consequently, we did not take RTs to be a direct proxy for the subjective experience of confidence. Nonetheless, it was important to verify that model-estimated confidence had a meaningful relationship with behavior in our task, that is, to the time it took participants to commit to a decision. An inverse quadratic relationship between behavioral RTs and model-estimated confidence would indicate that it took participants longer to commit to decisions that were associated with lower

degrees of model-estimated confidence. To test this, we fit RTs with mixed effects regression (lme4 package for R; [46]). Fixed effects specified the linear and quadratic extensions of value and a random effect on the model intercept was included to account for baseline variation in RT.

$$\bar{y} = b_0 + b_1(P(Acc) - P(Rej)) + b_2(P(Acc) - P(Rej))^2 + \varepsilon$$

Value predictors entered into the model were generated by sorting model-estimated value into 5 equally spaced bins and the dependent measures were participants' mean RTs for each bin. The model was tested again using z-scored SV as value predictors to verify that relationship between value and RTs were consistent regardless of the method used to estimate value.

Results

Behavioral choice models

A separate logistic regression model was fit to each participant's decisions to accept or reject shock/reward offers made while undergoing fMRI. All participants' model fits had significantly positive reward coefficients and significantly negative shock coefficients, indicating that both offer attributes influenced SV in the intended direction, despite individual differences in their relative contribution to choice outcomes (rewards: β_r estimates mean = .199, range = [0.064, 0.547], p values all $< .001$; costs β_s estimates: mean = -0.170, range = [-0.547, -0.050], p values all $< .001$) (Fig 2). Moreover, there was sizable variation in participants' model intercepts with ranges that spanned zero, suggesting strong individual differences in baseline tendencies to accept or reject offers (β_0 estimates: mean = 1.057, range = [-6.420, 9.750]). On average, participants tended to accept more offers than they rejected (mean = 61.3%, sd = 17.8%), and seemed to be engaged in the task (98.2% of all trials received responses before the 1.8s decision deadline).

GLM 1: Parametric modulation by SV and confidence

In GLM 1 we measured parametric modulation of BOLD responses by continuous regressors for SV and choice confidence over the course of value-based choices. Comprehensive lists of significant cluster activation from this and all following analyses are tabulated in S1 Table. During the offer phase SV correlated significantly with activation in many regions of cortex, including a network of value-related regions incorporating vmPFC, posterior cingulate cortex, orbitofrontal cortex (OFC) the basal ganglia, posterior insula, and hippocampus, as well as other regions known to be involved with perceptual and value comparison such angular gyrus, lateral temporal cortex, and visual cortex (Fig 3A).

We additionally found a relatively smaller set of regions where activity negatively correlated with confidence during the offer phase including areas associated with cognitive control and conflict resolution such as dACC and right lPFC, right superior parietal lobule (SPL), premotor regions, and visual cortex (Fig 3B). There were no voxels with activity negatively related with SV nor any voxels that were positively related with confidence during the offer phase. Notably, neural responses to neutral SV can't be easily interpreted with the SV regressor alone. Instead, the inverse of the confidence regressor can be interpreted as a measure of choice conflict. Both the dACC and lPFC demonstrated a strong inverse relationship with confidence, consistent with previous results demonstrating their recruitment during ambivalence, conflict, uncertainty, and choice difficulty during value based decision making and other tasks [21, 47–53]. The inverse relationship between the confidence regressor and conflict-resolution and positive relationship of the regressor with SV is compatible supports the idea that neural activity during the offer phase is primarily related to valuation processes.

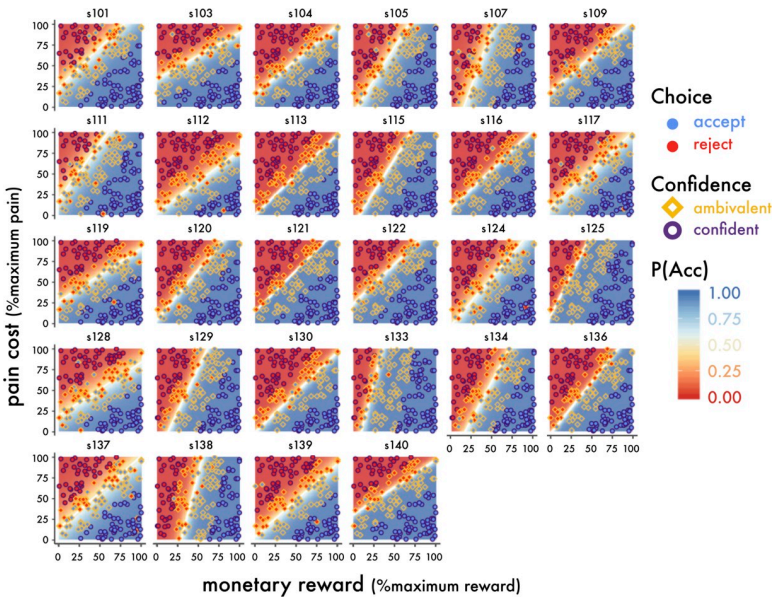

Fig 2. Observed decisions and model-based estimates of confidence and value. Individuals' choice outcomes are plotted over the decision space, which is shaded according to model-based P(Acc). Each coordinate is a possible offer, with the x-dimension representing percent maximum reward and the y-dimension representing the percent maximum pain cost. Observed choices are overlaid points, the filled color represents the observed decision (red = reject, blue = accept). The point outline represents model-based confidence (yellow = ambivalent, purple = confident). Decision boundaries are overlaid in white. There were substantial individual differences in choice behavior and model-estimated value, as well as differences in choice consistency (indicated by the width of the band of neutral color surrounding the decision boundary). Note that decision boundaries diverged considerably from the boundary of objective perceptual equality (the line of % maximum reward = % maximum pain, not illustrated), which comprises the set of offers for which the physical sizes of the cost and reward stimuli were identical.

https://doi.org/10.1371/journal.pone.0225617.g002

Surprisingly, we did not observe any BOLD responses, in vmPFC or elsewhere, that varied with SV during the commit phase. Furthermore, during the commit phase, there were no regions where activity varied negatively with choice confidence. Instead, choice confidence significantly predicted activity in a cluster of voxels within vmPFC as well as other regions including posterior insula, superior temporal cortex, and premotor areas during the commit phase (Fig 3C).

Assessment of first-level design matrices for GLM 1 revealed minimal multicollinearity between model terms. The mean R^2 between SV and confidence was 0.42 for both the offer and commit phases. While we thought it was valuable to examine this relationship, it is also important to note that structural collinearity, such as including a variable and its quadratic extension (i.e. SV and confidence), is not typically considered a design confound. Because the distributions of VIFs for SV and confidence were right-skewed, we report medians rather than means. For the offer phase, the median VIFs were 2.88 for the SV regressor and 2.94 for the confidence regressor. For the commit phase, the median VIFs were 2.90 for the SV regressor and 2.92 for the confidence regressor. In other domains, VIFs greater than 5 or 10 have traditionally been considered problematic, however to our knowledge there is no standard cutoff for fMRI designs [45]. We determined that the VIF of these regressors of interest was acceptably low, considering the structural collinearity between SV and confidence.

To characterize the dynamic relationship between SV and confidence signals in the vmPFC, we constructed an FIR model. As shown in Fig 4 beginning ~ 3 seconds after the presentation of an offer (consistent with a response delayed by the HRF), there is a rapid increase of SV related activity in vmPFC lasting approximately seven seconds. In contrast, activity

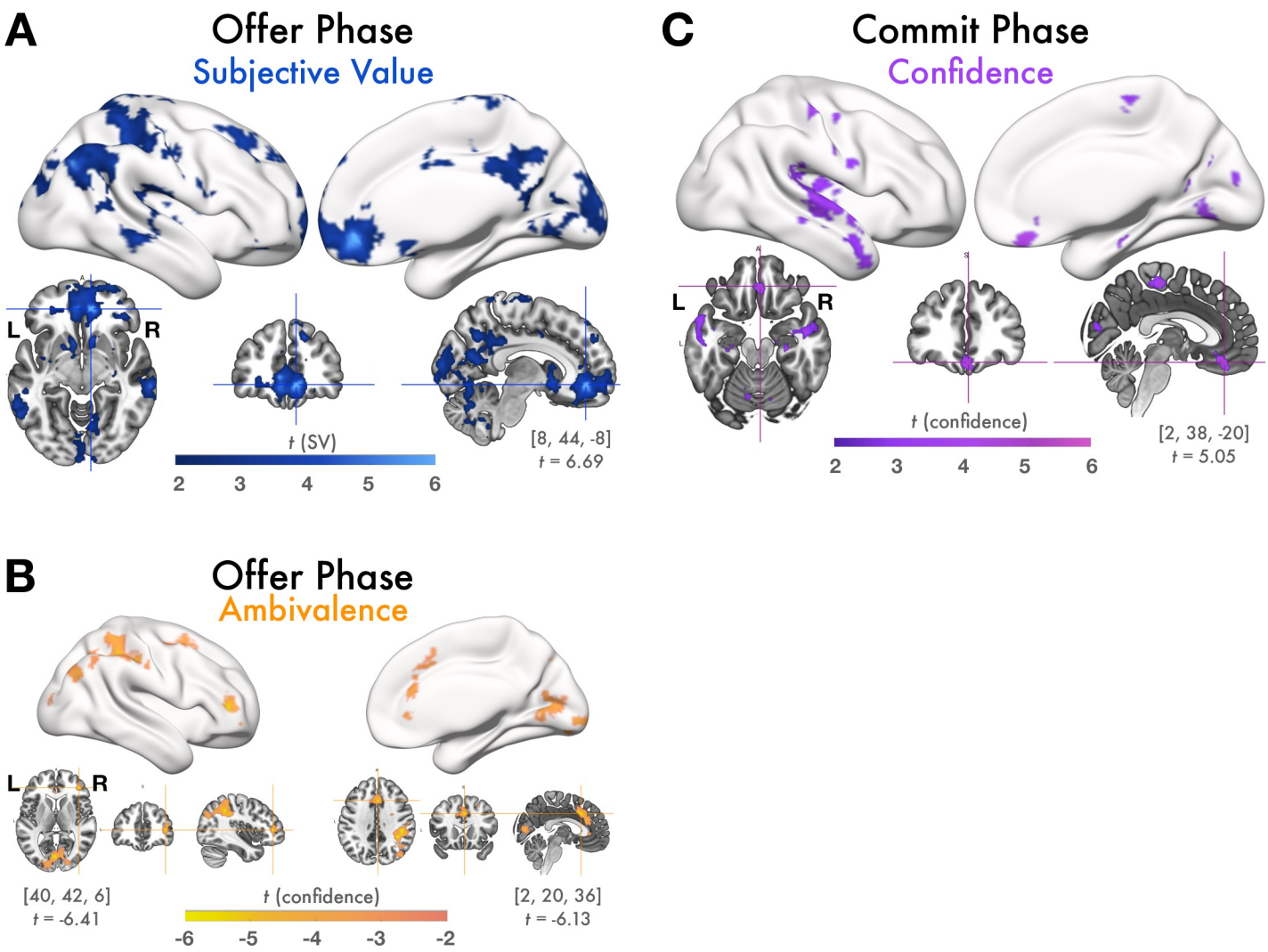

Fig 3. GLM1: Parametric correlation of BOLD with SV and confidence. During the offer phase, vmPFC tracked SV but not confidence and during the commit phase, vmPFC tracks confidence but not SV. Figures display all statistically significant results at $p < .05$ TFCE-corrected at the whole-brain level. **(A)** BOLD responses during the offer phase that correlated positively with model-estimated SV. During the offer phase, a large cluster of voxels in vmPFC tracked SV while participants evaluated the offer. Slice images show local peak activation in vmPFC, along with the MNI coordinates and t-value of the local maximum in this cluster. There was also significant activation throughout the value network including within posterior cingulate cortex, the basal ganglia, insula, and hippocampus; regions involved with value-comparison such as angular gyrus and lateral temporal cortex; and visual cortex. No voxels correlated positively with SV during the commit phase, suggesting that value-responses, particularly in vmPFC, emerge relatively early in the decision making process. **(B)** BOLD responses positively correlated with ambivalence (inversely correlated with confidence) during the offer phase. Areas involved with cognitive control and response competition, such as lPFC and dACC tracked ambivalence while participants deliberated accepting or rejecting the offer. Slice images show local maxima in regions of theoretical interest (lPFC and dACC). No voxels in vmPFC or elsewhere responded positively with choice confidence during the offer phase, suggesting that neural responses corresponding to high confidence emerge relatively later than SV and ambivalence. **(C)** BOLD responses correlated positively with model-estimated confidence during the commit phase. During the commit phase, while participants submitted a response and viewed feedback about their decision, a cluster of voxels in vmPFC tracked decision confidence, as well as regions including posterior insula and lateral temporal cortex. Slices images show peak activation in vmPFC.

https://doi.org/10.1371/journal.pone.0225617.g003

related to confidence emerges approximately 10 seconds after the offer (which is 5.5 seconds after the presentation of the response cue). As this activity reaches a peak around 13 seconds, SV related activity has already returned to baseline, demonstrating a clear cross-over in the timing of these two variables.

Taken together, the key finding from GLM1 was that whether estimated by classic HRF convolution or by FIR, vmPFC tracks SV but not confidence during the offer phase and confidence but not SV during the commit phase. These results suggest that in value-based decision

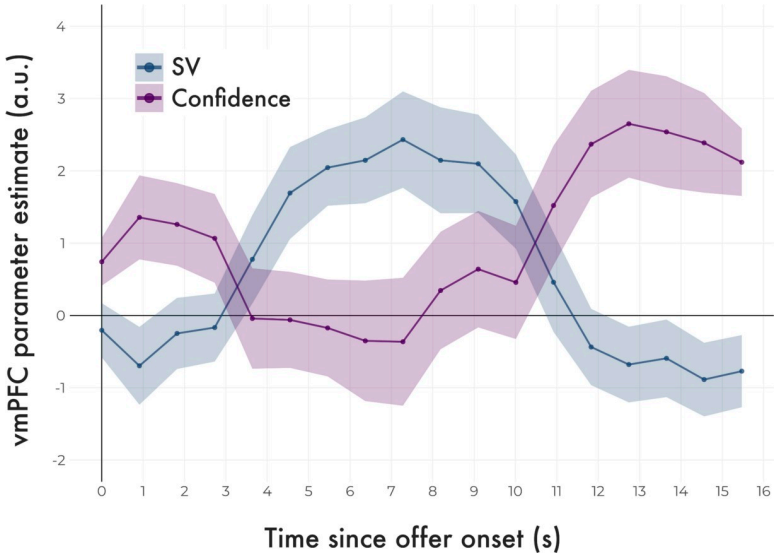

Fig 4. Time course of vmPFC responses tracking SV and confidence. SV signals preceded confidence signals in vmPFC. Neural responses were sampled once per TR (every 910 ms), beginning at the onset of the trial stimulus, marked here as 0 s. Plotted lines (group means) and ribbons (SEM) represent vmPFC parameter estimates over the course of the trial, estimated with an FIR model. The blue line traces the strength of the association between BOLD responses in vmPFC and model-estimated SV, the purple line traces their association with model-estimated confidence.

https://doi.org/10.1371/journal.pone.0225617.g004

making, vmPFC responses are modulated by both SV and confidence, but this does not appear to be a simultaneous process. Rather, there may be a temporal order to these signals such that vmPFC is first involved in the valuation process before transitioning to signaling confidence about that valuation. This interpretation supports the idea that vmPFC's dual roles in value-based decision making are more pronounced during separable stages of decision making.

GLM 2: Categorical choice by confidence conditions

While SV predicts choice outcomes (i.e. offers perceived as highly valuable are likely to be accepted), SV and outcome are not perfectly related, especially when choices are closer to one's decision boundary. It is possible that SV is computed relatively early on, but that vmPFC responses relating to the final choice (selected with respect to SV) occur later and concurrently with choice confidence, during the commit phase. Therefore, in GLM2 we measured responses related to choice outcomes and confidence. To do this, GLM2 modeled BOLD responses from four trial conditions: AccCon, RejCon, AccAmb, and RejAmb. These analyses mirror GLM1 except that in GLM2 value is signified as trial by trial choice outcome rather than estimated SV, and confidence is binned into high (confident) and low (ambivalent) categories. During the offer phase, we observed that a similar network of regions to those that were parametrically modulated by SV in GLM1 also showed significant contrasts for decision outcome in GLM2 such that BOLD responses were stronger preceding decisions to accept than decisions to reject (Fig 5A). This extends our findings from GLM1, demonstrating that not only SV but also a decision variable is represented within vmPFC relatively early in the decision making process, in this case during the offer phase.

There was substantial overlap between value-related responses in GLM1 and decisions to accept in GLM2. These similarities are likely attributable to participants' relatively stable choice behavior, causing SV model estimates to be strongly predictive of choice outcomes.

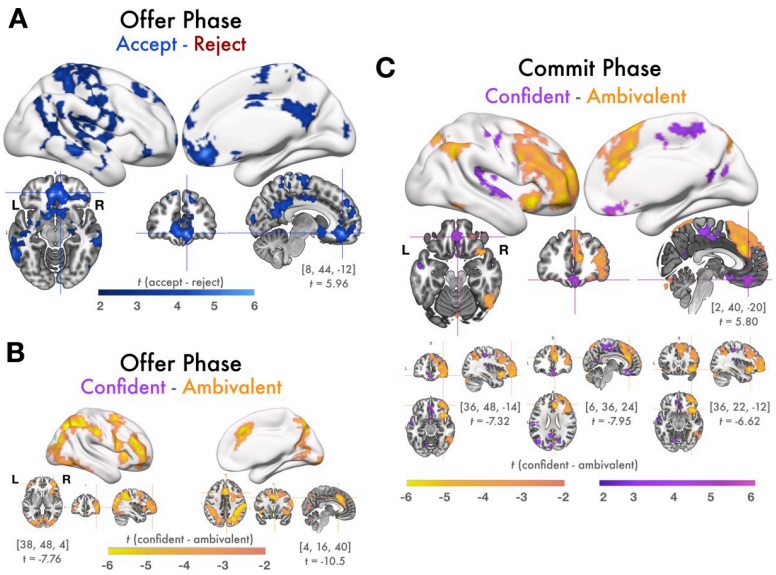

Fig 5. GLM2: Contrasts of decisions and confidence conditions. vmPFC encodes decision variables during the offer phase but not the commit phase, and encodes decision confidence during the commit phase, but not the offer phase. Figures display all statistically significant results at $p < .05$ TFCE-corrected at the whole-brain level. **(A)** Contrasts of response magnitudes from the offer phase of accept trials > reject trials: During the offer phase, clusters of voxels in vmPFC and other regions in the value network, many of which were also parametrically correlated with SV, had stronger response magnitudes preceding accept decisions than reject decisions. Slices images show peak coordinates in vmPFC. No voxels exhibited this contrast during the commit phase, nor were there any regions with stronger responses during rejected trials than accepted trials during either phase. **(B)** Contrasts of response magnitudes from the offer phase of confident trials < ambivalent trials. Slice images illustrate peak activation in lPFC and dACC. **(C)** Contrasts of response magnitudes from the commit phase of confident > ambivalent trials (purple) were observed in vmPFC were stronger for confident trials than ambivalent trials. No regions showed the same contrast during the offer phase. Clusters of voxels in lateral OFC, the anterior insula, and dACC showed the reverse pattern, with stronger response magnitudes during the commit phase of ambivalent trials than confident trials. Note that, several regions (dACC, lPFC, lateral OFC, and anterior insula) show the confident < ambivalent contrast during both the offer and commit phases. Slice images show peak coordinates for confident > ambivalent in vmPFC and peak coordinates for confident < ambivalent in lateral OFC, dACC, and anterior insula.

https://doi.org/10.1371/journal.pone.0225617.g005

Consequently, neural responses associated with high estimated SV in GLM1 were also observed duriinig accept choices in GLM2. The primary exception to this rule was visual cortex, where activity tracked SV but not choice outcome, suggesting that visual cortex activation varied with SV only insofar as it systematically related to visual properties of the offer stimuli.

Similarly, the contrast of BOLD responses from the offer phase of ambivalent versus confident choices revealed a similar network of regions as those that were negatively related to confidence during the offer phase from GLM1, with the addition of the anterior insula for GLM2 (Fig 5B). There were no regions, including vmPFC, with stronger responses during the offer phase of confident choices than the offer phase of ambivalent choices, nor were any regions more responsive during rejected trials than accepted trials.

During the commit phase, there were robust and widespread differences between confident and ambivalent choices, but no regions responded preferentially to one choice outcome (accept or reject) over the other. Critically, clusters of voxels in vmPFC as well as posterior cingulate, and an adjacent medial segment of superior parietal lobule showed a significant contrast between confident and ambivalent decisions during the commit phase, with stronger BOLD responses to confident choices (Fig 5C, purple). The reverse contrast (ambivalent versus confident) revealed several of the same regions that responded selectively to ambivalent choices during the offer phase, such as the anterior insula, lateral PFC, and dACC (Fig 5C,

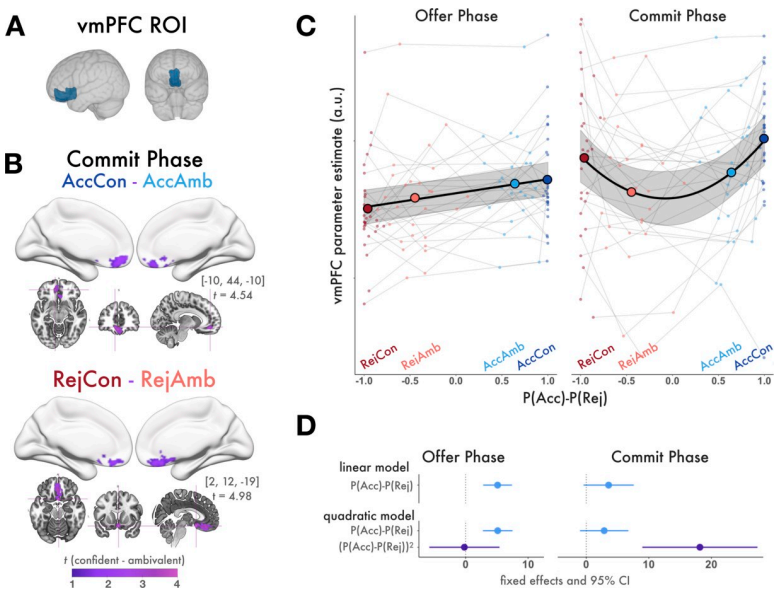

Fig 6. vmPFC ROI analysis. (A) Anatomical vmPFC ROI **(B)** AccCon > AccAmb and RejCon > RejAmb contrasts of BOLD responses during the commit phase. Figures display all statistically significant results at $p < .05$ TFCE-corrected within the vmPFC ROI. During the commit phase, vmPFC responses are stronger for high confidence choices, even for reject choices when confidence is inversely related with SV. **(C)** vmPFC Parameter estimates from the offer (left) and commit phase (right). Small points are individuals' raw vmPFC parameter estimates with respect to their mean P(Acc)-P(Rej) of each trial condition. Large points are group mean vmPFC parameter estimates with respect to the group mean P(Acc)-P(Rej) of each condition. The fit line indicates regression predictions and 95% CI from the winning model for that decision phase. During the offer phase, vmPFC responses increased linearly across trial conditions with increasing value. During the commit phase, they increased quadratically. **(D)** Comparison of mixed effects regression models predicting vmPFC parameter estimates (GLM2) from the and quadratic (bottom) extensions of value. Model estimates and 95% confidence intervals show fixed effects of linear and quadratic model terms, confidence intervals not spanning 0 are considered significant. vmPFC parameter estimates from the offer phase (left) were best fit with a linear model, indicating that during the offer phase, vmPFC tracks value. vmPFC parameter estimates from the commit phase (right) were best fit with a quadratic model, indicating that during the commit phase vmPFC tracks confidence.

https://doi.org/10.1371/journal.pone.0225617.g006

orange). This could possibly indicate sustained ambivalence-related activity that arises early in the valuation process and may still be unresolved at the time of choice commitment for highly difficult choices. The observed responses in vmPFC, which favored positive choice outcomes during the offer phase and high confidence during the commit phase, provide additional evidence of separable stages of activity over the course of a value-based choice.

Given the robust SV- (from GLM1) and choice-related (from GLM2) responses during the offer phase, it is possible that apparent confidence-related signals in vmPFC activity during the commit phase were in fact attributable to strong, sustained value-related responses carrying over from the offer phase. That is, relative differences in vmPFC responses to AccCon choices versus AccAmb choices could have driven the observed main effect of confidence–and moreover these effects might be better explained by value than confidence. To verify that the apparent effects of confidence could not be explained by relative differences in value, we measured contrasts of confident versus ambivalent BOLD responses separately for accepted and rejected offers. We were specifically interested in these comparisons within our a priori vmPFC ROI and therefore restricted statistical correction to this region alone (Fig 6A). During the commit phase, we observed a cluster of voxels with significantly stronger responses during RejCon versus RejAmb trials as well as a cluster of voxels that preferred AccCon to AccAmb (Fig 6B). Notably, because SV of RejCon trials is less than SV of RejAmb trials, this result suggests that

during the commit phase, clusters of vmPFC activity are signaling choice confidence irrespective of SV. We found no voxels that demonstrated the same pattern during the offer phase, nor did we find any voxels with stronger responses to ambivalent choices during either phase.

Time courses of SV and confidence responses in vmPFC

We examined the pattern of response magnitudes in vmPFC across trial conditions of increasing value and in both decision phases and compared the fits of models with linear and quadratic terms (Fig 6C). For the offer phase, the linear model best explained the observed pattern of vmPFC parameter estimates across the four conditions as the additional term in the quadratic model did not improve the model fit (Linear model: AIC = 901.1, BIC = 911.98; Quadratic model: AIC = 903.1, BIC = 916.69; comparison of models: $\chi2(1) = .0018$, $p = .966$), indicating that vmPFC activity increased linearly with P(Acc)-P(Rej) during the offer phase (signaling value). For the commit phase, the quadratic model best explained the observed pattern of vmPFC parameter estimates (Linear model: AIC = 1014.5, BIC = 1025.3, Quadratic Model: AIC = 1002, BIC = 1015.6, comparison of models: $\chi2(1) = 14.320$, $p < .001$), indicating that vmPFC responses take a quadratic function with respect to value during the commit phase (signaling confidence). Model effects are plotted in Fig 6D and details about model fits are shown in Table 1.

In summary, vmPFC responses increased linearly across trial conditions of increasing value during the offer phase, signifying early involvement with valuation of the offer stimulus, and varied quadratically across the same conditions during the commit phase, signifying late involvement with valuation of the decision and deriving confidence. Notably, no values associated with model-estimated confidence (such as those used in GLM1) were entered into the

Table 1. Comparison of linear mixed models estimating vmPFC responses from value.

	Fixed Effects					Random Effect	Model Fit				Model Comparison	
	Estimate	95CI		*t*	*p*	*SD*	Marg. R^2	Cond. R^2	AIC	BIC	$\chi2$	*p*
Offer: Linear Model						14.58	0.05	0.70	901.1	912.0		
Intercept	-19.08	-24.74	-13.28	-6.56	<0.001							
P(accept)-P(reject)	5.10	2.73	7.41	4.38	<0.001							
Offer: Quadratic model						14.57	0.05	0.70	903.1	916.7	0.002	0.966
Intercept	-19.00	-25.78	-12.20	-5.50	<0.001							
P(accept)-P(reject)	5.11	2.76	7.40	4.33	<0.001							
$(P(accept)-P(reject))^2$	-0.12	-5.76	5.44	-0.04	0.967							
Commit: Linear Model						19.17	0.01	0.55	1014.5	1025.3		
Intercept	-9.07	-17.08	-1.02	-2.28	0.031							
P(accept)-P(reject)	3.63	-0.48	7.78	1.76	0.082							
Commit: Quadratic model						19.18	0.07	0.61	1002.0	1015.6	14.43	< 0.001
Intercept	-20.86	-30.57	-10.96	-4.20	<0.001							
P(accept)-P(reject)	2.87	-0.96	6.63	1.49	0.140							
$(P(accept)-P(reject))^2$	18.16	9.21	27.27	3.91	<0.001							

Results of model comparisons estimating vmPFC responses from value. The first column identifies the model and variables specified as fixed effects from that model. Columns 2–6 give the model estimate, 95% confidence interval (95CI), and t statistic and p value estimated from Satterthwaite approximation. Column 7 is the standard deviation (SD) of the random effect (Intercept | Subject). Columns 8–11 are overall model statistics: variance explained by fixed effects (Marg. = marginal R^2), variance explained by fixed and random effects together (Cond. = conditional R^2), and overall model AIC, and BIC. The final two columns are with $\chi2$ statistics and p values from likelihood ratio tests (after refitting models with maximum likelihood estimates), describing improvement of fit from adding quadratic term to the original linear model.

https://doi.org/10.1371/journal.pone.0225617.t001

mixed effects models. Rather, the models estimated participants' mean parameter estimates from the four trial conditions (of GLM2) from their mean P(Acc)-P(Rej) for all trials of that condition. Therefore, the plots in Fig 6C demonstrate that during the offer phase, vmPFC responses naturally take a linear function across the four trial conditions of ascending value P (Acc)-P(Rej), whereas during the commit phase, vmPFC responses naturally take a quadratic function across the same trial conditions.

Strictly speaking, because P(Acc)-P(Rej) takes a sigmoid function with respect to SV and that vmPFC increased linearly with SV in GLM1, vmPFC responses could theoretically take a logistic function with respect to P(Acc)-P(Rej). Visual inspection of individual raw vmPFC parameter estimates (Fig 6B) did not reveal that the underlying pattern of vmPFC parameter estimates had a logistic shape. To verify that this was the case, we repeated the linear mixed regression model, substituting SV predictors for P(Acc)-P(Rej) predictors, and found analogous statistical results. While the fMRI parameter estimates had sufficient resolution to discern between linear and quadratic functions, it is unlikely that a similar distinction could be made between two monotonic functions such as linear and logistic functions. We present results with respect to P(Acc)-P(Rej) because this measure improved the interpretability of group-wide results by controlling the range of predictor values across the group while preserving the sign of raw SV, as described in the methods above.

Temporally restricted value and confidence signals in vmPFC. An additional analysis tested for the temporal dissociation of value and confidence processing within in vmPFC. We took the conjunction of vmPFC voxels with activation during the offer phase that was significantly stronger for accept decisions than reject decisions and activation during the commit phase that was significantly stronger for confident decisions than ambivalent decisions, excluding common terms between the contrasts. This revealed cluster of voxels within vmPFC that switched from value-selective activation during the offer phase to confidence-selective activation during the commit phase (Fig 7).

Behavioral RTs and confidence

Before analysis, trials with RTs exceeding 3 SD of the overall group mean were excluded (1.56%). Additionally, trials exceeding 3 SD of the individual's mean RT for each bin of each analysis were excluded (0.98%). The model confirmed that RTs took an inverse quadratic function with respect to value (Fixed Effects: (P(Acc)-P(Rej) estimate = -35.415, 95CI [-50.042, -20.787], SE = 7.466, t = -4.743, $p < .001$; P(Acc)-P(Rej)^2 estimate = -77.330, 95CI [-102.213, -52.451], SE = 12.700, t = -6.90, $p <. 001$; Random Effect SD = 88.02), indicating that participants were slower to commit to decisions associated with low model-estimated confidence (Fig 8). Notably, in addition to the quadratic relationship, there was also a negative linear correlation between value and RTs, indicating that it took participants longer to commit to decisions about low value offers versus high value offers. This may have been caused by the observed bias for accept decisions over reject decisions, which meant that responses to lower value offers required overriding the default decision to accept.

We observed statistically analogous, but somewhat weaker results when using SV as value predictors (Fixed Effects: SV estimate = -27.198, 95CI [-32.326, -22.070], SE = 2.618, t = -10.390, $p < .001$; SV^2 estimate = -7.900, 95CI [-12.230, -3.563], SE = 2.212, t = -3.570, p = .001; Random Effect SD = 8.020), which is likely due to large individual differences in estimated SV, as described above. Taken together, the results of the RT analysis confirmed that there was a meaningful relationship between model-estimated confidence and behavior. Participants were slower to commit to decisions about offers we predicted would elicit ambivalence, suggesting that these choices might have been more challenging to resolve. This is not

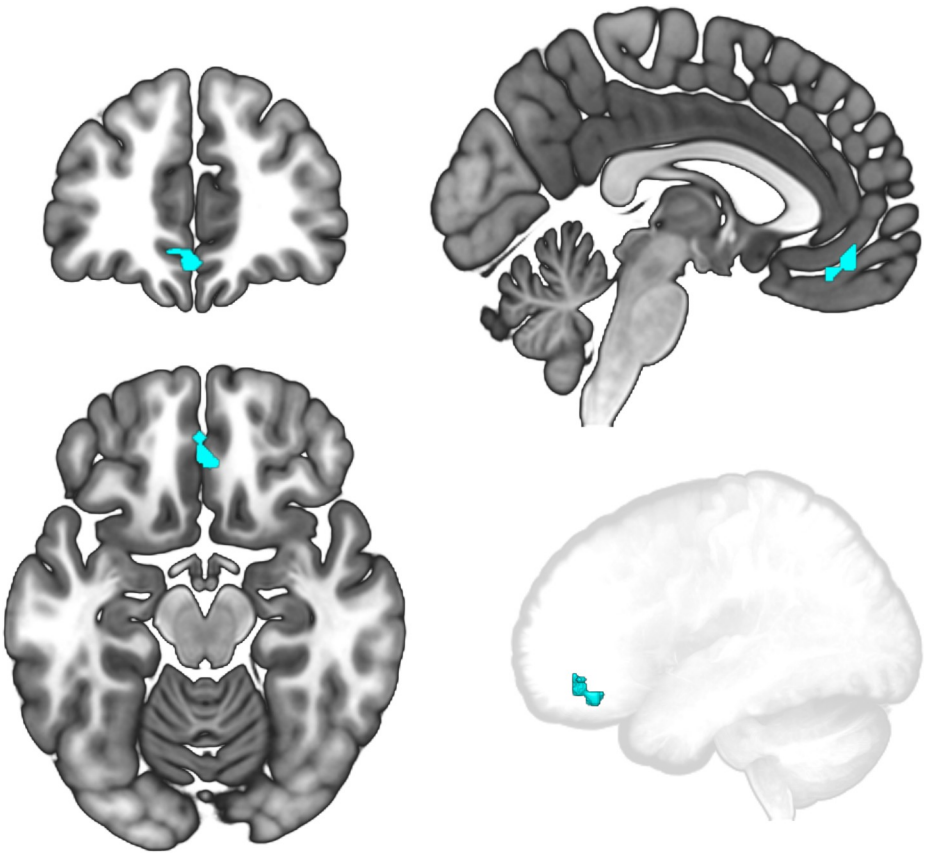

Fig 7. Conjunction of offer phase value responses and commit phase confidence responses. vmPFC voxels that were sensitive to value during the offer phase and to confidence during the commit phase are shown in slices images and in a glass brain. These voxels had significant contrasts for AccAmb > RejCon during the offer phase and for RejCon > AccAmb during the commit phase ($p < .05$ TFCE-corrected within the anatomical vmPFC ROI), and therefore switched from tracking offer valuation to tracking decision confidence during the sequential decision phases.

https://doi.org/10.1371/journal.pone.0225617.g007

an indication that RTs measure the subjective experience of confidence, but rather that there is an empirical basis that model-estimated confidence captures aspects of our task associated with decision difficulty. Importantly, because participants varied in their subjective preferences and their decision boundaries diverged considerably from the reward = cost line (Fig 2), increased RTs for ambivalent choices cannot be explained by difficulty in perceptual discrimination (i.e. merely determining whether costs or rewards were perceptually larger).

Discussion

We measured behavioral and neural responses during a two-phase Ap-Av decision making task with consequential mixed outcomes. Model-based SV, confidence estimates and decision variables correlated with BOLD responses throughout the cortex, including within vmPFC. Our series of results provides strong support for the recent suggestion that vmPFC encodes both value and confidence during value-based decision making [17, 19, 21]. Importantly, the present research is the first evidence of this phenomena in the realistic context of deterministic approach avoidance choice scenarios. It extends previous findings from studies that have used different approaches for assessing confidence, including explicit rating of hypothetical SV for items or events [17], deciding between two positively-items [19], or decisions with

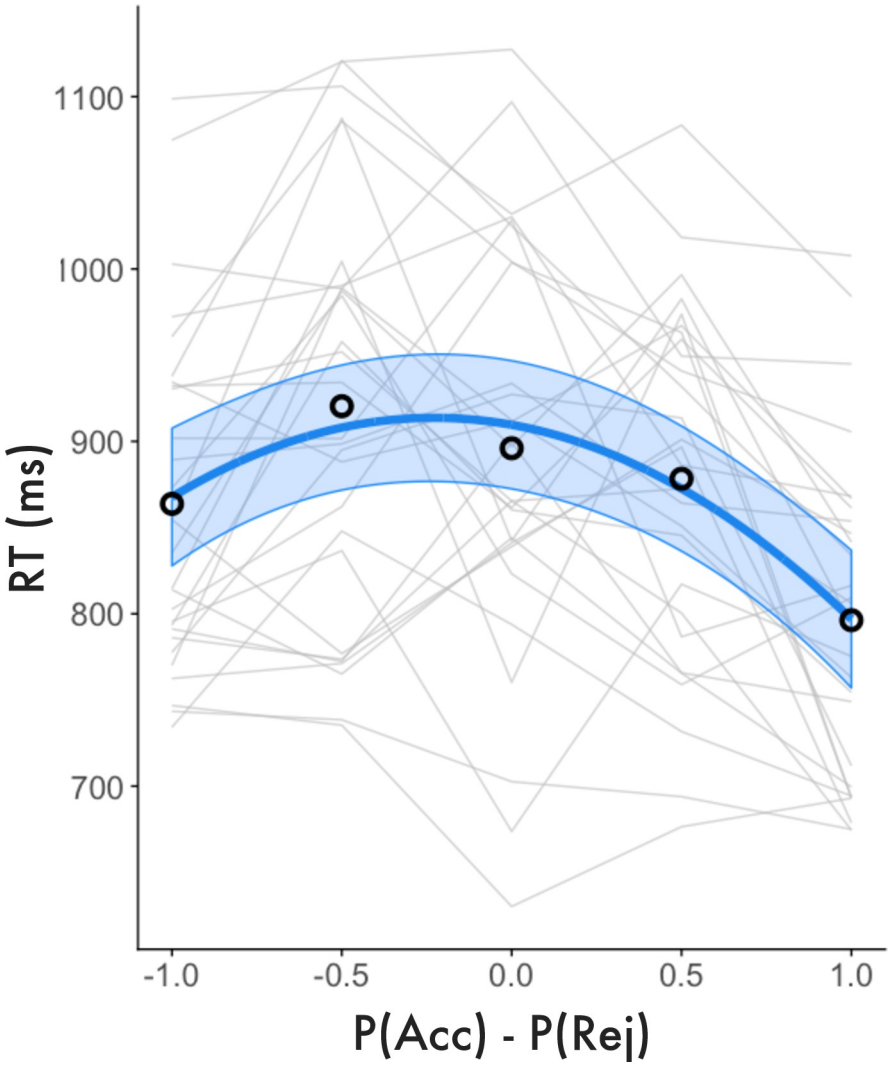

Fig 8. RT analysis. Individual and group mean RTs (small lines) are plotted with respect to value (P(Acc)-P(Rej)). Fit lines represent model predicted RTs and 95% CIs. RTs take an inverse quadratic function with respect to model-estimated value. The time it took participants to commit to decisions was negatively correlated with model-estimated confidence (the quadratic extension of value).

https://doi.org/10.1371/journal.pone.0225617.g008

probabilistic risk [21]. We then presented novel evidence that such vmPFC signals have a temporal order within the course of decision making. Specifically, vmPFC activation tracked offer valuation (SV) and choice determination early in the trial as participants deliberated their decision and tracked decision valuation (confidence) relatively later. The following sections discuss our key findings regarding neural signatures of SV and confidence as well limitations of this study and suggestions for future research.

Early value responses in vmPFC

Our first finding was new evidence of approach-selective vmPFC responses preceding choice commitment in an economic ApAv task. During the offer phase of each trial, participants deliberated on accepting or rejecting offers and vmPFC responses increased with estimated SV (GLM1). We complemented this finding by demonstrating that parameter estimates from an

anatomical vmPFC ROI increased monotonically with P(Acc)-P(Rej) (GLM2), consistent with a vast literature documenting vmPFC's role in integrating items' cost and reward attributes into its overall SV [4, 11, 12, 54]. vmPFC also distinguished between decision outcomes during the offer phase, with stronger responses anticipating accept decisions than reject decisions (GLM2). These results may be partially explained by goods-based models of value-based decision making, which propose that economic choices are made between goods rather than actions [55], and can therefore be settled prior to planning the action to submit the decision [56].

Remarkably, we found no regional activation that was significantly modulated by SV (GLM1) or that differed by choice outcome (GLM2) during the commit phase, even when statistical correction was restricted to vmPFC (GLM2). This result was unexpected given previous findings that vmPFC representations of subjective preferences are automatically elicited by task stimuli, including contexts in which such information is task-irrelevant [7, 57]. Moreover, SV responses in vmPFC can sustain the entire presentation of value stimuli with durations far longer than the time needed to make a decision, regardless of whether the additional time affects decision behavior [58]. Together, these prior findings suggested that in our study, vmPFC would encode SV whenever the offer stimuli were visible, including during the commit phase. One possible explanation for why we did not find such effects is that we implemented a two-phase decision task whereas other paradigms require immediate responses, only briefly present value stimuli, or rapidly transition from choice commitment to decision outcomes. A two-phase decision task may better accommodate observation and analysis of the temporal ordering of offer valuation and decision valuation processes within vmPFC.

An alternative hypothesis is that there were in fact enduring but relatively weak SV representations in vmPFC during the commit phase that did not reach statistical significance. Inspection of the group mean vmPFC parameter estimates during the commit phase (GLM2) suggests a somewhat asymmetrical quadratic function such that accepted offers, on average, were associated with larger response magnitudes than rejected offers. However, a linear model provided only a marginal fit to the same data, consistent with only a subtle positive correlation, if any, between vmPFC activation and value during the commit phase. Nonetheless, these observations left open the possibility that vmPFC continued to track offer value, albeit weakly, through the commit phase, even if this effect was markedly exceeded by confidence. To obtain more direct evidence of a temporal dissociation between value and confidence processing during decision making, we conducted a conjunction analysis (GLM2 conjunction), which revealed a cluster of vmPFC voxels that switched from value-selective activation while participants evaluated the offer to confidence-selective activation as participants committed to a decision and received feedback. This result, which does not rely on interpreting null effects as evidence of absence, lends strong support for the conclusion that value and confidence processing within vmPFC temporally dissociate.

Late confidence responses in vmPFC

There have been various empirical and theoretical suggestions that confidence signals emerge early in decision making, evolving in parallel with processing of choice stimuli and the decision itself [17, 22, 23, 59]. Others have reported evidence that confidence lags behind decision variables and value estimates, emerging closer to the time of choice commitment or even later [25, 27–32]. We presented a series of results that converged to decidedly endorse the latter, and to our knowledge provide the first evidence for delayed confidence processing in the context of value-based decision making.

Specifically, we did not observe any BOLD responses that were parametrically correlated with confidence during the offer phase (GLM1) nor any regional activation during the offer

phase that was selective for confident over ambivalent choices (GLM2), even when statistical correction was restricted to vmPFC. Instead, it was during the commit phase of the decision process, while participants submitted a choice and received feedback, that vmPFC responses increased parametrically with decision confidence (GLM1) and similarly were stronger for confident choices than ambivalent choices (GLM2). Inspection of vmPFC parameter estimates from the commit phase revealed a quadratic function with respect to increasing value (GLM2). Therefore, during the commit phase, vmPFC responses were stronger for confident choices than ambivalent choices, even for rejected offers when high confidence is associated with low SV. Visualization of the time course SV and confidence responses in vmPFC (GLM1 FIR) illustrated a distinct temporal order of early value-related signal and late confidence-related signal in vmPFC. It is noteworthy that the SV and confidence regressors peaked at similar delays following the onset of the offer stimulus and response cue, respectively. While the delay of the BOLD response makes it difficult to identify precisely when in the trial this transition occurred, this may be preliminary evidence that the most robust confidence-related response was triggered by the cue for the participant to commit a response.

Neuroanatomical substrates of value and confidence

Beyond vmPFC, we observed extensive overlap between regions that parametrically correlated with SV during the offer phase (GLM1) and regions that preferentially activated during the offer phase of accept decisions compared with reject decisions (GLM2). This was observed in a larger value-network including regions important for sensory association, value-comparison, and reward processing such as angular gyrus, posterior parietal cortex, lateral temporal cortex, posterior cingulate cortex, and the ventral striatum. The value network likely encodes finer-grained distinctions between SV and choice outcome than were apparent in our analyses. For example, others have suggested separable time courses for evolving value signals and decision variables [60]. Our paradigm was well suited for SV and confidence signals but not necessarily for dissociating SV from decision variables, given the strong correlation between the two. Future research aiming to find finer dissociations of SV and decision variables may benefit from novel variations of our task.

Furthermore, our anatomical vmPFC ROI was selected a priori and is somewhat inclusive, combining subcallosal cortex and medial frontal cortex from the Harvard-Oxford atlas, which comprise structures that others have labeled medial OFC, pregenual or subgenual ACC. Thus, we cannot draw meaningful conclusions about functional or temporal specificity at a smaller scale but we appreciate that others have made interesting discoveries on this front. For example, it has been suggested that over the course of stimulus processing, OFC is the first cortical site where appetitive stimuli are assigned reward, whereas later processing in vmPFC transforms value representations into choices [54] that guide action selection [61]. Another recent study found a spatial gradient of information processing in mPFC with ventral regions responding more strongly to value and dorsal regions responding more strongly to confidence [62]. Interestingly, we did not observe the same pattern. In our analyses, the most robust confidence effects were observed in ventral and posterior portions of mPFC surrounding subgenual ACC and the most robust SV and approach-selective effects were observed relatively dorsal and anterior within mPFC, closer to the frontal pole. One possible explanation for this discrepancy is that De Martino and colleagues' task [62] enabled participants to incorporate other individuals' value ratings into confidence judgments, which may have recruited theory of mind processing in dorsomedial prefrontal cortex [63]. Other previous research that employed a strategy game requiring choices to attack or defend reported that an adjacent region, rostral ACC, preferentially responded when participants defended versus attacked and tracked the

value of deploying defense strategies but not attack strategies [10]. While we did not observe regional activation that correlated negatively with SV nor regions that selectively responded to reject choices, the conceptual equivalent to defending, the notion of separable but adjacent neural bases for approach and avoidance behaviors is compelling. Combining finer parcellation of prefrontal cortex with fMRI models that include terms for individual offer attributes reveal separable patterns of responses to reward, SV, and choice outcome may be an interesting avenue for future research. However, this was beyond the scope of our study.

Implicit choice confidence

It has been previously demonstrated that model-based confidence estimates correspond closely to self-reported confidence [17] and the strength of the relationship between model-based confidence and vmPFC activation strongly predicts the relationship between self-reported confidence and vmPFC activation [15]. A key aspect of our study was the characterization of confidence without a reliance on post-hoc self-report or metacognition. Using a naturalistic task and implicit measures of confidence, we replicated previous findings that model-estimated confidence had an inverse quadratic relationship with RTs [17], such that increasing model-estimated confidence predicted faster decision commitments (Fig 7), suggesting that model-estimated confidence captures an element of choice difficulty.

A similar study by De Martino et al. [19], which incorporated explicit confidence ratings with an fMRI value-based choice task suggests separable neural signals corresponding to model-based and self-reported confidence and found that while vmPFC tracked unsigned value differences between choice options (which roughly correspond to our model-estimated confidence), rostrolateral PFC (rlPFC) tracked self-reported confidence. They used this basis to ground a hypothesis that rlPFC probes internal confidence signals, represented in vmPFC, and makes them available for metacognitive self-report. Others have made similar claims [64]. Notably, rlPFC responses correlated with ambivalence in our task (which did not require explicit confidence ratings), suggesting that our task did not elicit similar metacognitive appraisal processes. While there is not yet broad consensus regarding the loci of implicit versus metacognitive confidence–it seems evident that decision tasks requiring metacognitive confidence judgments may recruit unique neural resources from tasks that model confidence directly from decision behavior. Nonetheless, our results support recent suggestions that implicit confidence, the valuation of one's judgment, shares a neuroanatomical basis with a variety of other valuation processes, vmPFC [17, 20, 30]. We add to this growing theoretical framework evidence for a dynamic process by which vmPFC shifts from valuation of external stimuli to valuation of internal value representations and the decisions they inspire.

Supporting information

S1 Table. Significant cluster activation from GLM1 and GLM2. Full details of significant task-related activation. Clusters <10 voxels excluded. The first three columns identify the analysis, decision phase when BOLD responses were measured, and the variable measured in the statistic (Con. = confiden(t)ce, Amb. = ambivalen(t)ce. The next column specifies each cluster and indicates the total number of voxels in that cluster. The remaining columns are details about local maxima within that cluster, including t-value (* signifies cluster peaks illustrated in figures), MNI coordinates, region from AAL of MNI space, and Brodmann area (- signifies peak voxel falls outside of labelled cortex, region provided is the closest).
(XLSX)

Acknowledgments

This work supported by Grant W911NF-16-1-0474, Contract W911NF-09-0001 and Cooperative Agreement W911NF-19-2-0026 with the Army Research Office of the Army Research Laboratory. We thank Mario Mendoza, Gold Okafor, and Viktoriya Babenko for their assistance with data collection as well as Neil Dundon, Michelle Marneweck, Tyler Santander, and Evan Layher for helpful suggestions.

Author Contributions

Conceptualization: Allison D. Shapiro, Scott T. Grafton.

Data curation: Allison D. Shapiro.

Formal analysis: Allison D. Shapiro.

Funding acquisition: Scott T. Grafton.

Investigation: Allison D. Shapiro.

Methodology: Scott T. Grafton.

Supervision: Scott T. Grafton.

Writing – original draft: Allison D. Shapiro.

Writing – review & editing: Scott T. Grafton.

References

1. Rangel A, Camerer C, Montague PR. A framework for studying the neurobiology of value-based decision making. Nat Rev Neurosci. 2008 Jun 11; 9(7):545–56. https://doi.org/10.1038/nrn2357 PMID: 18545266
2. Bartra O, McGuire JT, Kable JW. The valuation system: A coordinate-based meta-analysis of BOLD fMRI experiments examining neural correlates of subjective value. NeuroImage. Elsevier Inc; 2013 Aug 1; 76(C):412–27.
3. Basten U, Biele G, Heekeren HR, Fiebach CJ. How the brain integrates costs and benefits during decision making. Proc Natl Acad Sci USA. 2010 Dec 14; 107(50):21767–72. https://doi.org/10.1073/pnas.0908104107 PMID: 21118983
4. Amemori K-I, Graybiel AM. Localized microstimulation of primate pregenual cingulate cortex induces negative decision-making. Nat Neurosci. 2012 Apr 8; 15(5):776–85. https://doi.org/10.1038/nn.3088 PMID: 22484571
5. Levy DJ, Glimcher PW. The root of all value: a neural common currency for choice. Current Opinion in Neurobiology. Elsevier Ltd; 2012 Dec 1; 22(6):1027–38. https://doi.org/10.1016/j.conb.2012.06.001 PMID: 22766486
6. Talmi D, Pine A. How Costs Influence Decision Values for Mixed Outcomes. Front Neurosci. 2012; 6.
7. Lebreton M, Jorge S, Michel V, Thirion B, Pessiglione M. An Automatic Valuation System in the Human Brain: Evidence from Functional Neuroimaging. Neuron. Elsevier Ltd; 2009 Nov 12; 64(3):431–9. https://doi.org/10.1016/j.neuron.2009.09.040 PMID: 19914190
8. Pessiglione M, Delgado MR. The good, the bad and the brain: neural correlates of appetitive and aversive values underlying decision making. Current Opinion in Behavioral Sciences. 2015; 5:78–84. https://doi.org/10.1016/j.cobeha.2015.08.006 PMID: 31179377
9. Skvortsova V, Palminteri S, Pessiglione M. Learning To Minimize Efforts versus Maximizing Rewards: Computational Principles and Neural Correlates. Journal of Neuroscience. 2014; 34(47):15621–30. https://doi.org/10.1523/JNEUROSCI.1350-14.2014 PMID: 25411490
10. Wan X, Cheng K, Tanaka K. Neural encoding of opposing strategy values in anterior and posterior cingulate cortex. Nat Neurosci. 2015 Apr 20; 18(5):752–9. https://doi.org/10.1038/nn.3999 PMID: 25894290
11. Talmi D, Dayan P, Kiebel SJ, Frith CD, Dolan RJ. How Humans Integrate the Prospects of Pain and Reward during Choice. Journal of Neuroscience. 2009 Nov 18; 29(46):14617–26. https://doi.org/10.1523/JNEUROSCI.2026-09.2009 PMID: 19923294

12. Park SQ, Kahnt T, Rieskamp J, Heekeren HR. Neurobiology of Value Integration: When Value Impacts Valuation. Journal of Neuroscience. 2011 Jun 22; 31(25):9307–14. https://doi.org/10.1523/JNEUROSCI.4973-10.2011 PMID: 21697380

13. Heereman J, Walter H, Heekeren HR. A task-independent neural representation of subjective certainty in visual perception. Front Hum Neurosci. 2015 Oct 9; 9(e96511):195–12.

14. Gherman S, Philiastides MG. Human VMPFC encodes early signatures of confidence in perceptual decisions. eLife. 2018; 7.

15. Bang D, Fleming SM. Distinct encoding of decision confidence in human medial prefrontal cortex. Proc Natl Acad Sci USA. National Academy of Sciences; 2018 Jun 5; 115(23):6082–7. https://doi.org/10.1073/pnas.1800795115 PMID: 29784814

16. Hebscher M, Barkan-Abramski M, Goldsmith M, Aharon-Peretz J, Gilboa A. Memory, Decision-Making, and the Ventromedial Prefrontal Cortex (vmPFC): The Roles of Subcallosal and Posterior Orbitofrontal Cortices in Monitoring and Control Processes. Cereb Cortex. 2016 Dec; 26(12):4590–601. https://doi.org/10.1093/cercor/bhv220 PMID: 26428951

17. Lebreton M, Abitbol R, Daunizeau J, Pessiglione M. Automatic integration of confidence in the brain valuation signal. Nat Neurosci. 2015 Aug; 18(8):1159–67. https://doi.org/10.1038/nn.4064 PMID: 26192748

18. Rolls ET, Grabenhorst F, Deco G. Choice, difficulty, and confidence in the brain. NeuroImage. 2010; 53(2):694–706. https://doi.org/10.1016/j.neuroimage.2010.06.073 PMID: 20615471

19. De Martino B, Fleming SM, Garrett N, Dolan RJ. Confidence in value-based choice. Nat Neurosci. 2013 Jan; 16(1):105–10. https://doi.org/10.1038/nn.3279 PMID: 23222911

20. Hebscher M, Gilboa A. A boost of confidence: The role of the ventromedial prefrontal cortex in memory, decision-making, and schemas. Neuropsychologia. 2016; 90:46–58. https://doi.org/10.1016/j.neuropsychologia.2016.05.003 PMID: 27150705

21. Schlund MW, Brewer AT, Magee SK, Richman DM, Solomon S, Ludlum M, et al. The tipping point: Value differences and parallel dorsal-ventral frontal circuits gating human approach-avoidance behavior. NeuroImage. 2016 Aug 1; 136:94–105. https://doi.org/10.1016/j.neuroimage.2016.04.070 PMID: 27153979

22. Dotan D, Meyniel F, Dehaene S. On-line confidence monitoring during decision making. Cognition. Elsevier; 2018 Feb 1; 171:112–21. https://doi.org/10.1016/j.cognition.2017.11.001 PMID: 29128659

23. Kepecs A, Uchida N, Zariwala HA, Mainen ZF. Neural correlates, computation and behavioural impact of decision confidence. Nature. 2008 Aug 10; 455(7210):227–31. https://doi.org/10.1038/nature07200 PMID: 18690210

24. Kiani R, Corthell L, Shadlen MN. Choice Certainty Is Informed by Both Evidence and Decision Time. Neuron. Elsevier Inc; 2014 Dec 17; 84(6):1329–42.

25. Pleskac TJ, Busemeyer JR. Two-stage dynamic signal detection: a theory of choice, decision time, and confidence. Psychological Review. 2010 Jul; 117(3):864–901. https://doi.org/10.1037/a0019737 PMID: 20658856

26. van den Berg R, Anandalingam K, Zylberberg A, Kiani R, Shadlen MN, Wolpert DM. A common mechanism underlies changes of mind about decisions and confidence. eLife. 2016 Feb 1; 5:e12192. https://doi.org/10.7554/eLife.12192 PMID: 26829590

27. Moran R, Teodorescu AR, Usher M. Post choice information integration as a causal determinant of confidence: Novel data and a computational account. Cognitive Psychology. Elsevier Inc; 2015 May 1; 78(C):99–147.

28. Resulaj A, Kiani R, Wolpert DM, Shadlen MN. Changes of mind in decision-making. Nature. Nature Publishing Group; 2009 Oct 9; 461(7261):263–6. https://doi.org/10.1038/nature08275 PMID: 19693010

29. Yu S, Pleskac TJ, Zeigenfuse MD. Dynamics of postdecisional processing of confidence. Journal of Experimental Psychology: General. 2015 Apr; 144(2):489–510.

30. Fleming SM, van der Putten EJ, Daw ND. Neural mediators of changes of mind about perceptual decisions. Nat Neurosci. 2018 Apr 1; 21(4):617–24. https://doi.org/10.1038/s41593-018-0104-6 PMID: 29531361

31. Hilgenstock R, Weiss T, Witte OW. You'd Better Think Twice: Post-Decision Perceptual Confidence. NeuroImage. Elsevier Inc; 2014 Oct 1; 99(C):323–31.

32. Morales J, Lau H, Fleming SM. Domain-General and Domain-Specific Patterns of Activity Supporting Metacognition in Human Prefrontal Cortex. Journal of Neuroscience. 2018 Apr 4; 38(14):3534–46. https://doi.org/10.1523/JNEUROSCI.2360-17.2018 PMID: 29519851

33. Volz LJ, Welborn BL, Gobel MS, Gazzaniga MS, Grafton ST. Harm to self outweighs benefit to others in moral decision making. Proc Natl Acad Sci USA. 2017; 114(30):7963–8. https://doi.org/10.1073/pnas.1706693114 PMID: 28696302

34. Amemori KI, Amemori S, Graybiel AM. Motivation and Affective Judgments Differentially Recruit Neurons in the Primate Dorsolateral Prefrontal and Anterior Cingulate Cortex. Journal of Neuroscience. 2015 Feb 4; 35(5):1939–53. https://doi.org/10.1523/JNEUROSCI.1731-14.2015 PMID: 25653353

35. Cieslak M, Ryan WS, Macy A, Kelsey RM, Cornick JE, Verket M, et al. Simultaneous acquisition of functional magnetic resonance images and impedance cardiography. Psychophysiol. John Wiley & Sons, Ltd (10.1111); 2015 Apr; 52(4):481–8.

36. Avants BB, Tustison NJ, Song G, Cook PA, Klein A, Gee JC. A reproducible evaluation of ANTs similarity metric performance in brain image registration. NeuroImage. 2011; 54(3):2033–44. https://doi.org/10.1016/j.neuroimage.2010.09.025 PMID: 20851191

37. Smith SM. Fast robust automated brain extraction. Hum Brain Mapp. 2002 Nov; 17(3):143–55. https://doi.org/10.1002/hbm.10062 PMID: 12391568

38. Jenkinson M, Bannister P, Brady M, Smith S. Improved Optimization for the Robust and Accurate Linear Registration and Motion Correction of Brain Images. NeuroImage. 2002 Oct; 17(2):825–41. https://doi.org/10.1016/s1053-8119(02)91132-8 PMID: 12377157

39. Jenkinson M, Smith S. A global optimisation method for robust affine registration of brain images. Med Image Anal. 2001 Jun; 5(2):143–56. https://doi.org/10.1016/s1361-8415(01)00036-6 PMID: 11516708

40. Andersson JLR, Jenkinson M, Smith SM. Non-linear optimisation. FMRIB technical report. 2007.

41. Andersson JLR, Jenkinson M, Smith SM. Non-linear registration, aka Spatial normalisation. 2007.

42. Woolrich MW, Ripley BD, Brady M, Smith SM. Temporal Autocorrelation in Univariate Linear Modeling of FMRI Data. NeuroImage. 2001 Dec; 14(6):1370–86. https://doi.org/10.1006/nimg.2001.0931 PMID: 11707093

43. Nichols TE, Holmes AP. Nonparametric permutation tests for functional neuroimaging: a primer with examples. Hum Brain Mapp. 2002 Jan; 15(1):1–25. https://doi.org/10.1002/hbm.1058 PMID: 11747097

44. Winkler AM, Ridgway GR, Webster MA, Smith SM, Nichols TE. Permutation inference for the general linear model. NeuroImage. The Authors; 2014 May 15; 92(C):381–97.

45. Mumford JA, Poline J-B, Poldrack RA. Orthogonalization of Regressors in fMRI Models. Ben Hamed S, editor. PLoS ONE. 2015 Apr 28; 10(4):e0126255–11. https://doi.org/10.1371/journal.pone.0126255 PMID: 25919488

46. Bates D, Mächler M, Bolker BM, Walker SC. Fitting linear mixed-effects models using lme4. Journal of Statistical Software. 2015 Jan 1; 67(1).

47. Badre D, Doll BB, Long NM, Frank MJ. Rostrolateral prefrontal cortex and individual differences in uncertainty-driven exploration. Neuron. 2012 Feb 9; 73(3):595–607. https://doi.org/10.1016/j.neuron.2011.12.025 PMID: 22325209

48. Lopez-Persem A, Domenech P, Pessiglione M. How prior preferences determine decision-making frames and biases in the human brain. eLife. 2016 Nov 19; 5:2308.

49. Aupperle RL, Melrose AJ, Francisco A, Paulus MP, Stein MB. Neural substrates of approach-avoidance conflict decision-making. Hum Brain Mapp. 2015 Feb; 36(2):449–62. https://doi.org/10.1002/hbm.22639 PMID: 25224633

50. Shenhav A, Straccia MA, Botvinick MM, Cohen JD. Dorsal anterior cingulate and ventromedial prefrontal cortex have inverse roles in both foraging and economic choice. Cognitive, Affective, & Behavioral Neuroscience. 2016; 16(6):1127–39.

51. Economides M, Guitart-Masip M, Kurth-Nelson Z, Dolan RJ. Anterior cingulate cortex instigates adaptive switches in choice by integrating immediate and delayed components of value in ventromedial prefrontal cortex. Journal of Neuroscience. 2014 Jan 1; 34(9):3340–9. https://doi.org/10.1523/JNEUROSCI.4313-13.2014 PMID: 24573291

52. Shenhav A, Straccia MA, Cohen JD, Botvinick MM. Anterior cingulate engagement in a foraging context reflects choice difficulty, not foraging value. Nat Neurosci. 2014 Sep 1; 17(9):1249–54. https://doi.org/10.1038/nn.3771 PMID: 25064851

53. Kahnt T, Heinzle J, Park SQ, Haynes J-D. Decoding different roles for vmPFC and dlPFC in multi-attribute decision making. NeuroImage. 2011 May; 56(2):709–15. https://doi.org/10.1016/j.neuroimage.2010.05.058 PMID: 20510371

54. Grabenhorst F, Rolls ET. Value, pleasure and choice in the ventral prefrontal cortex. Trends in Cognitive Sciences. 2011 Feb; 15(2):56–67. https://doi.org/10.1016/j.tics.2010.12.004 PMID: 21216655

55. Padoa-Schioppa C, Assad JA. Neurons in the orbitofrontal cortex encode economic value. Nature. 2006 May 11; 441(7090):223–6. https://doi.org/10.1038/nature04676 PMID: 16633341

56. Wunderlich K, Rangel A, O'Doherty JP. Economic choices can be made using only stimulus values. Proc Natl Acad Sci USA. National Academy of Sciences; 2010 Aug 24; 107(34):15005–10. https://doi.org/10.1073/pnas.1002258107 PMID: 20696924

57. Smith DV, Hayden BY, Truong T-K, Song AW, Platt ML, Huettel SA. Distinct value signals in anterior and posterior ventromedial prefrontal cortex. Journal of Neuroscience. 2010 Feb 17; 30(7):2490–5. https://doi.org/10.1523/JNEUROSCI.3319-09.2010 PMID: 20164333

58. Sokol-Hessner P, Hutcherson C, Hare T, Rangel A. Decision value computation in DLPFC and VMPFC adjusts to the available decision time. Eur J Neurosci. 2012 Apr; 35(7):1065–74. https://doi.org/10.1111/j.1460-9568.2012.08076.x PMID: 22487036

59. Gherman S, Philiastides MG. Neural representations of confidence emerge from the process of decision formation during perceptual choices. NeuroImage. 2015 Feb 1; 106:134–43. https://doi.org/10.1016/j.neuroimage.2014.11.036 PMID: 25463461

60. Rushworth MF, Kolling N, Sallet J, Mars RB. Valuation and decision-making in frontal cortex: one or many serial or parallel systems? Current Opinion in Neurobiology. Elsevier Ltd; 2012 Dec 1; 22(6):946–55. https://doi.org/10.1016/j.conb.2012.04.011 PMID: 22572389

61. Rushworth MF, Mars RB, Summerfield C. General mechanisms for making decisions? Current Opinion in Neurobiology. 2009 Feb; 19(1):75–83. https://doi.org/10.1016/j.conb.2009.02.005 PMID: 19349160

62. De Martino B, Bobadilla-Suarez S, Nouguchi T, Sharot T, Love BC. Social Information Is Integrated into Value and Confidence Judgments According to Its Reliability. Journal of Neuroscience. Society for Neuroscience; 2017 Jun 21; 37(25):6066–74. https://doi.org/10.1523/JNEUROSCI.3880-16.2017 PMID: 28566360

63. Lee D. Decision Making: From Neuroscience to Psychiatry. Neuron. Elsevier Inc; 2013 Apr 24; 78 (2):233–48. https://doi.org/10.1016/j.neuron.2013.04.008 PMID: 23622061

64. Fleming SM, Huijgen J, Dolan RJ. Prefrontal contributions to metacognition in perceptual decision making. Journal of Neuroscience. 2012 May 2; 32(18):6117–25. https://doi.org/10.1523/JNEUROSCI.6489-11.2012 PMID: 22553018